

Effect of Hole Trapping on the Microscopic Structure of Oxygen Vacancy Sites in α -SiO₂[†]

Andrew C. Pineda*

Albuquerque High Performance Computing Center, The University of New Mexico, 1601 Central Avenue, NE (Galles Building), Albuquerque, New Mexico 87131

Shashi P. Karna*

U.S. Air Force Research Laboratory, Space Vehicles Directorate, 3550 Aberdeen Avenue, SE, Building 914, KAFB, New Mexico 87117-5776

Received: November 17, 1999; In Final Form: February 10, 2000

To develop an improved fundamental understanding of the microscopic effects of hole trapping by oxygen vacancy sites (V_O) in amorphous α -SiO₂, we have performed ab initio Hartree–Fock calculations of the structure and energy of model silicon dioxide clusters. Three different precursor clusters were employed in these calculations: (A) a 15-atom cluster without rings; (B) a 39-atom cluster containing four 6-atom (3-membered) rings; and (C) an 87-atom cluster with four 12-atom (6-membered) rings. For clusters A and B, a double- ζ plus polarization (DZP) basis set was used. For cluster C, a minimal (STO-3G) basis set was employed. Our results suggest that the energy of formation, ΔE_f of V_O in the neutral (V_O^0) and positive (V_O^{+1}) charge states depends on the starting size and geometry of the precursor. Similarly, microscopic structural changes, primarily network relaxation, due to hole trapping by V_O^0 strongly depend on the initial local structure around the vacancy. A neutral vacancy, V_O^0 , tends to form a Si–Si dimer bond regardless of the network structure. Similarly, hole trapping at V_O in a relatively rigid network containing 6-atom (3-membered) fused rings results in a small, but symmetric relaxation (i.e., elongation) of the Si–Si bond at the vacancy site. When the network contains more flexible structures, such as 12-atom (6-membered) rings adjacent to V_O and sufficient asymmetry, trapping of a hole causes an asymmetric relaxation of the two adjacent Si atoms. The asymmetric relaxation in our calculation proceeds without a barrier. The value of ΔE_f for V_O^0 and V_O^{+1} decreases with the flexibility and asymmetry in the oxide network.

Introduction

Charge trapping by thin amorphous silicon dioxide (α -SiO₂) films is one of the major sources of performance degradation of metal oxide semiconductor (MOS) devices. Therefore, much effort has been expended in the past three decades to understand the microscopic mechanism of charge trapping and its effects on the physics of MOS devices. Experimental evidence suggests that oxygen vacancy sites (V_O) in the dielectric α -SiO₂ layer of MOS structures are the primary hole trap sites.^{1,2} Although the exact mechanism of hole trapping by V_O remains unknown, it is widely accepted that network relaxation leading to the creation of deep trap levels in the SiO₂ band gap is one of the consequences of charge trapping. The latter phenomenon causes a long-term buildup of oxide-trapped positive charge. However, the exact nature of the network relaxation that results in the long-term buildup of oxide charge following charge trapping remains unknown to date.

According to a popular model, proposed by Feigl, Fowler, and Yip³ (FFY) a quarter of a century ago, trapping of a hole by a V_O in α -quartz causes an asymmetric relaxation of the Si atoms adjacent to the vacancy. Specifically, the hole is localized on a silicon atom that moves away from its original position in the vacancy through the plane of its three adjoining oxygen atoms where it is stabilized by bonding to an oxygen atom from the surrounding network while an unpaired electron is localized

on another 3-fold coordinated silicon atom that essentially remains fixed at its original position in the vacancy. The unpaired electron occupies one of the dangling sp^3 bonds of the undisplaced silicon atom. This model, which was originally proposed to explain the observation of electron spin resonance (ESR) detection of a V_O center in α -quartz known as the E'_1 center, is widely used to explain the formation mechanism and local atomic structure of a related defect center, known as the E'_γ center, in α -SiO₂. Although never verified experimentally, the most appealing feature of the FFY model lies in its ability to provide a physical basis to explain the localization of the unpaired electron spin following hole trapping on a single silicon atom, as evidenced from the ESR spectrum of the E'_γ center.

The FFY model is supported by quantum mechanical semiempirical calculations within the cluster approach⁴ and density functional theory (DFT) calculations within the super cell approach,⁵ which suggest that upon hole trapping, a V_O relaxes asymmetrically with a lowering of the total energy of the system by about 0.3–0.4 eV. The DFT calculations also suggest that the asymmetric relaxation of the network does not occur spontaneously after hole trapping by V_O , but rather the process involves an energy barrier of about 0.1–0.4 eV.⁵

Despite its widespread appeal, the FFY model fails to explain a number of important features related to charge trapping at V_O in α -SiO₂, or its charge state. One such example is the ESR observation of the E'_δ center.^{6–10} Recent ab initio quantum mechanical calculations,^{11,12} performed on model SiO₂ clusters,

[†] Part of the special issue "Electronic and Nonlinear Optical Materials: Theory and Modeling".

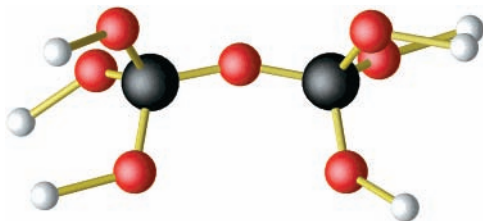


Figure 1. Precursor cluster A. Optimized geometry for the 15-atom precursor cluster. The large atoms are silicon atoms, the medium atoms are oxygen atoms, and the smallest atoms are hydrogen atoms. Bonds are shown for bond orders greater than 0.5.

have established this center to be a hole trapped at a simple mono-oxygen vacancy site. The E'_δ center results from a hole trapped at a V_O in which the unpaired electron spin is shared equally by two silicon atoms. The hole trapping in this case causes a “symmetric relaxation” that leads to a slight increase in the internuclear distance between the two Si atoms adjacent to the relaxed neutral V_O . This suggests that asymmetric relaxation of the SiO_2 network is not the only effect caused by hole trapping at a V_O center in $\alpha\text{-SiO}_2$.

The FFY model also fails to describe the neutral E' centers, also known as hemi- E' (E'_h) centers, in $\alpha\text{-SiO}_2$.^{13–15} Their ESR features, including the characteristic resonance position of the spectrum, the g -tensor, and the electron spin–nuclear spin hyperfine coupling tensor, are remarkably close to those observed for the E'_γ centers. The experiments and ab initio quantum mechanical calculations agree on the fact that the unpaired electron is localized on a dangling sp^3 bond at a 3-fold coordinated silicon center. It is therefore not clear whether hole trapping is a necessary condition for the observation of the so-called E'_γ centers, since the charge states of these defects have never been unambiguously established.

In light of these facts, it is important to develop an improved understanding of the microscopic effects of charge trapping by V_O centers in $\alpha\text{-SiO}_2$. It is clear, however, that the present model of the charge trapping by V_O does not fully account for all known effects. Therefore, it is important to develop a more comprehensive understanding of the effect of charge trapping by V_O in $\alpha\text{-SiO}_2$. To gain such an understanding, we have performed ab initio Hartree–Fock calculations on model SiO_2 clusters of varying size and geometrical features. Attention is focused on (a) the energy of V_O formation, ΔE_f , in the neutral and positive charge state and (b) changes in the structural features following hole trapping by V_O .

Our results suggest that both ΔE_f and the structural changes for V_O^q ($q = 0, +1$) depend on the starting local structure of the SiO_2 network. The technical details of the calculations are described in the following section. Subsequently, the results of the calculation are presented and discussed. The main findings of the study are then summarized in the conclusion.

Calculations

Precursor Calculations. The precursor clusters used to generate the model mono-oxygen vacancy clusters in the present study are shown in Figures 1–3. The largest spheres in the figures represent the silicon atoms, the medium spheres represent the oxygen atoms, and the smallest spheres represent hydrogen atoms. The hydrogen atoms were used to saturate the valency of the outer oxygen atoms. Cluster A (Figure 1) is the simplest model for a two-silicon center while clusters B and C essentially model Si–O networks of increasing size and flexibility. Model cluster B (Figure 2a) consists of two fused pairs of 6-atom rings with alternating Si–O bonds (or in the parlance of the solid

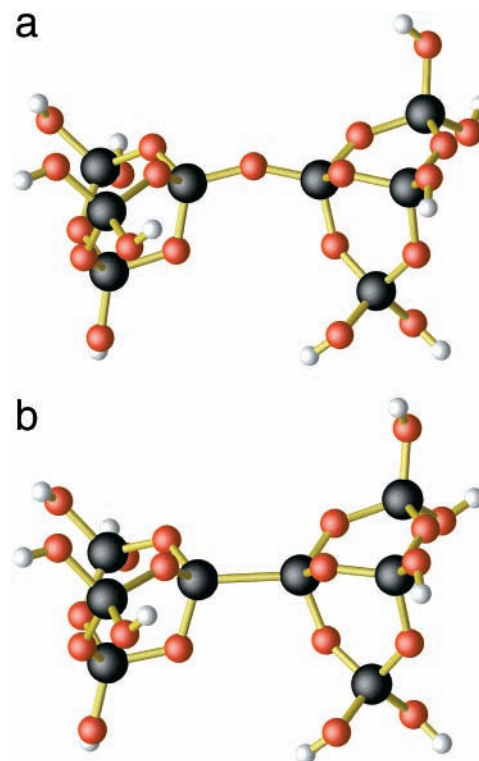


Figure 2. (a) Precursor cluster B. Optimized geometry for the 39-atom precursor cluster. The large atoms are silicon atoms, the medium atoms are oxygen atoms, and the smallest atoms are hydrogen atoms. Bonds are shown for bond orders greater than 0.5. (b) Model vacancy $V_O^0(B)$. Optimized geometry for the model 38-atom, neutral, 2-silicon center mono-oxygen vacancy, V_O . Bonds are shown for bond orders greater than 0.5.

state community, fused pairs of 3-member rings where “member” refers only to the number of silicon atoms in the rings) bridged by a single oxygen atom. Cluster C (Figure 3a) consists of two fused pairs of 12-atom (6-member) rings bridged by a single oxygen atom. The optimized geometries of the neutral precursor clusters A and B were taken from our previous studies.^{11,12} These were obtained by an ab initio restricted Hartree–Fock (RHF) calculation using a double- ζ Cartesian Gaussian basis set augmented by a six-component d polarization function on silicon and oxygen atoms and a three-component p polarization function on the hydrogen atoms. The optimized geometry of the precursor cluster C was obtained by a RHF calculation using a minimal (STO-3G) basis set. All atoms were allowed to move in the optimizations. Calculations were performed using the GAMESS electronic structure code.¹⁶

Charged and Neutral Mono-Oxygen Vacancy Calculations. Models for neutral mono-oxygen vacancies (V_O^0) were generated by removing the bridging oxygen atom connecting the two central silicon atoms in the precursor clusters and then optimizing the resulting structures via an ab initio RHF calculation. As in the precursor case, the small and medium neutral vacancy models, $V_O^0(A)$ and $V_O^0(B)$, were optimized using a double- ζ plus polarization (DZP) basis set that included p and d polarization functions and the large neutral model cluster, $V_O^0(C)$, was optimized using a minimal (STO-3G) basis set. Positively charged mono-oxygen vacancies (V_O^{+1}) were similarly generated by removing the bridging oxygen atom and an electron, and then optimizing the resulting structures via an ab initio unrestricted Hartree–Fock (UHF) calculation using the same basis sets as were employed in the neutral case. Again, all atoms in the clusters were allowed to move in the optimizations.

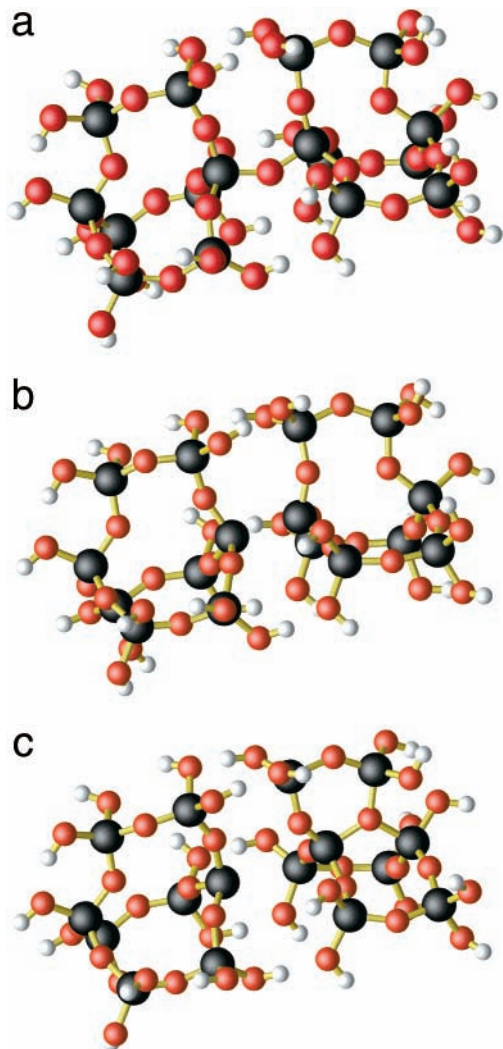


Figure 3. (a) Precursor cluster C. Optimized geometry for the 87-atom precursor cluster. The large atoms are silicon atoms, the medium atoms are oxygen atoms, and the smallest atoms are hydrogen atoms. Bonds are shown for bond orders greater than 0.5. (b) Model vacancy $V_O^0(C)$. Optimized geometry for the model 86-atom, neutral, 2-silicon center mono-oxygen vacancy, V_O . Bonds are shown for bond orders greater than 0.5. (c) Model vacancy $V_O^{+1}(C)$. Optimized geometry for the model 86-atom, positively charged, 2-silicon center mono-oxygen vacancy, V_O^{+1} . Note that one of the central silicon atoms has migrated outward and bonded to an oxygen atom in the outer network.

Distortions of the neutral and positively charged vacancies about their respective equilibrium geometries were also studied by adding or removing an electron to the optimized positive and neutral vacancies and optimizing the structures again. If no spontaneous relaxation of the positively charged cluster occurred in the course of the geometry optimization, then a silicon atom from the vacancy was moved into the adjoining network in order to attempt to locate a second energy minimum. The specific details of these calculations will be discussed on a case by case basis in the next section.

Results

Information about the local structure of the precursors and optimized neutral vacancies are summarized in Tables 1 and 2, respectively. After forming the neutral vacancies from the precursors by removing the bridging oxygen atom, the two central silicon atoms in all cases moved into the vacancy site (see Figures 2b and 3b) and formed bonds between 2.33 and

TABLE 1: Structural Parameters Adjoining Vacancy Site for RHF Calculations on Precursor Clusters

model cluster	A ^a	B	C
R_{Si-Si} (Å)	3.089	3.119	3.077
R_{Si-O} (Å) (adjoining center)	1.625	1.623–1.638	1.583–1.624
R_{Si-O} (Å) (all)	1.621–1.624	1.603–1.646	1.583–1.697
$\angle Si-O$ (central)–Si (deg)	170	153.740	146.182
E (hartree)	–1105.961 598	–3891.533 817	–7909.281 697
basis set	DZP	DZP	STO-3G

^a Reference 11.

TABLE 2: Structural Parameters Adjoining Vacancy Site for RHF Calculations on Optimized Neutral Vacancies

model vacancy (V_O)	$V_O^0(A)$	$V_O^0(B)$	$V_O^0(C)$
R_{Si-Si} (Å)	2.351	2.331	2.438
R_{Si-O} (Å) (adjoining center)	1.635	1.6334–1.6504	1.608–1.641
R_{Si-O} (Å) (all)		1.604–1.6504	1.587–1.696
$\angle O-Si(1)-O$ (deg)		104.510	108.714
		109.794	107.045
		103.706	106.982
$\angle O-Si(2)-O$ (deg)		108.778	105.542
		104.001	107.630
		104.507	108.555
E (hartree)	–1030.950 265	–3816.521 002	–7835.368 618
basis set	DZP	DZP	STO-3G

TABLE 3: Important Structural Parameters for UHF Calculations Optimized Positively Charged Vacancies

model positive vacancy (V_O^+)	$V_O^+(A)$ ^a	$V_O^+(B)$	$V_O^+(C)$
R_{Si-Si} (Å)	2.798	2.650	3.766
$R_{Si(1)-O}$ (Å) (no. of atoms)	1.587	1.582–1.604 (3)	1.624–1.646 (3)
$R_{Si(2)-O}$ (Å) (no. of atoms)	1.587	1.588–1.602 (3)	1.561–1.759 (4)
R_{Si-O} (Å) (all)	n/a	1.582–1.681	1.561–1.759
$\angle O-Si(1)-O$		110.812	106.384
		118.676	107.028
		109.662	107.722
$\angle O-Si(2)-O$		117.434	113.946
		110.328	115.787
		110.613	99.555
			115.848
			105.908
			103.068
$\rho^0_{Si(1)}, \rho^0_{Si(2)}$	0.2740, 0.2730	0.3016, 0.3214	0.4380, –0.0005
E (hartree)	–1030.662 080	–3816.193 912	–7835.252 629
$E - E(V_O)$ (eV)	7.8421	8.9007	3.1563
basis set	DZP	DZP	STO-3G

^a Reference 11.

2.44 Å in length, in good accord with literature data for a Si–Si bond.^{11,17} The bond lengths for the Si–O bonds are approximately 1.6 Å for all the clusters, both neutral and charged, we have studied. As the size of the clusters increases, the range of observed Si–O bond lengths observed increases slightly. The Si–Si bond distance in the precursors is largest in the medium cluster (Figure 2a), probably owing to steric effects arising from the relative rigidity of that cluster. The O–Si–O bond angles in the neutral vacancy models are in general smaller than the tetrahedral bond angle of 109°, indicating that most of the decrease in distance between the silicon atoms is due to motion of the atoms adjacent to the vacancy rather than motion of the two halves of the cluster toward each other.

Information about the local structure of the optimized positively charged vacancy models are summarized in Table 3. When the positively charged vacancies were formed by the removal of the bridging oxygen and an electron from the

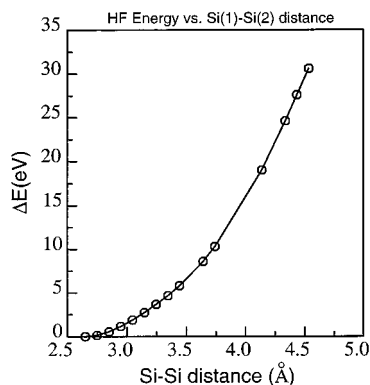


Figure 4. Hartree–Fock energy vs Si(1)–Si(2) distance as Si(1) is distorted outward from its equilibrium position in the model positively charged, 2-silicon center, mono-oxygen vacancy, $V_O^{+1}(B)$. The remaining atoms are held fixed. The lines in the figure are guides to the eyes.

corresponding precursors, different behavior was observed depending upon the availability of an oxygen atom from the surrounding network for binding and upon the flexibility of the surrounding oxide network. In the case of the small and medium vacancies, $V_O^{+1}(A)$ and $V_O^{+1}(B)$, the two central silicon atoms also move into the vacancy site, again forming a dimer, albeit with a longer bond distance on the order of 2.7 Å. The spin density on the central silicon atoms remains approximately equal, indicating that the two silicon atoms are equivalent. The O–Si–O bond angles around the two central silicon atoms are basically tetrahedral, but with a significant distortion in the case of the medium vacancy, $V_O^{+1}(B)$, since the ring structure is not symmetric. In an attempt to locate a second minimum geometry for $V_O^{+1}(B)$, one of the silicon atoms was moved in a line through the three neighboring oxygen atoms and the energies calculated with the remaining atoms held fixed. The energies obtained are shown in Figure 4. The energies are found to rise rapidly as bonds are bent and shortened. Similar, but less dramatic rises in energy occur for the small cluster, $V_O^{+1}(A)$.

We allowed $V_O^{+1}(B)$ to seek another minimum energy configuration by carrying out a geometry optimization starting from a puckered configuration in which one of the central silicon atoms was placed within the oxide network while the remaining atoms were left at their locations within the optimized positive vacancy. In this case, the silicon atom spontaneously moves back into the vacancy after only a few iterations of the geometry optimization, suggesting that the dimer is the only locally stable minimum energy configuration. Boero and co-workers⁵ have noted that this is the case when no suitable oxygen candidate is available to stabilize the puckered configuration.

In the case of the large positively charged vacancy model, $V_O^{+1}(C)$, the geometry is found to spontaneously distort with one silicon atom bonding to an oxygen atom in the network (Figure 3c), moving slightly over an angstrom from its original position toward one of the oxygen atoms in the surrounding network. The spin density is found to localize on the silicon atom remaining in the vacancy site. In Table 4, we estimate the stability of the large neutral, $V_O^0(C)$, and positive, $V_O^{+1}(C)$, vacancies at their optimized geometries with respect to the removal and addition of an electron. We find an energy difference on the order of 3 eV for both neutral and positively charged vacancies at the two optimized geometries. No indication of a barrier between the two configurations was observed during the optimization.

TABLE 4: Energy Changes Associated with Relaxation after Adding or Removing an Electron from the Neutral and Positively Charged Large Vacancies (Model $V_O(C)$) at Their Respective Optimized Geometries at the STO-3G Level

structure	energy (hartree)	relative energy, $E - E_{opt}$ (eV)
V_O^+ at V_O (opt geometry)	−7835.148 516	2.8331
V_O at V_O^+ (opt geometry)	−7835.238 161	3.5500

Discussion

A clearer picture of the mechanism of V_O^q ($q = 0, +1$) formation emerges from the results presented here. It is first noted that in all cases, the post- V_O formation relaxation of the network results in the formation of a Si–Si dimer bond whereby the two Si atoms adjacent to the V_O move inward. The calculated Si–Si bond in V_O^0 is somewhat larger in model C, which may be due to the use of a relatively poor basis set. This observation is consistent with previous semiempirical and ab initio calculations.^{4,11,17}

Trapping of a hole by V_O^0 in all three clusters results in a lengthening of the Si–Si bond distance relative to that of the relaxed V_O^0 . Upon placing a positive charge on V_O^0 , the two Si atoms in the case of models A and B move slightly away from each other. However, the Si–Si distance in both cases A and B is still about 0.3–0.5 Å shorter than that prior to the formation of the vacancy. In contrast, a density functional theory (DFT) calculation in super cell approximation⁵ suggests that the Si atoms adjacent to V_O^{+1} always “move away” from the vacancy; i.e., the Si–Si distance is always greater than the Si–Si distance prior to the formation of the vacancy. We consider this result of ref 5 to be wrong and perhaps caused by the approximations used in the calculation. The reason for this is not apparent to us; however, it is clear that the method used by these authors is incapable of adequately describing a localized charged defect in amorphous material. In fact, Boero et al.⁵ also obtain an incorrect description of the equivalent defect in the crystalline SiO_2 (quartz), where the Si–Si bond length in the case of V_O^{+1} is nearly the same as prior to the vacancy formation.

Unlike model A and B, the cluster in model C relaxes asymmetrically upon placing a positive charge on V_O^0 . The corresponding increase in $R(\text{Si–Si})$ in the case of asymmetric relaxation, $V_O(C)$, is over 1.3 Å. We note that one of the Si atoms adjacent to V_O moves away from its original position in the V_O^0 to a position inside the network to form a weak bond with a nearby O atom. The spatial location of this O atom, which is pointing inside one of the 6-member rings, facilitates the puckering of the system.

In model $V_O(A)$ with no rings beyond the second nearest-neighbor (NN) O atoms (with respect to the missing bridging oxygen) and in model $V_O(B)$ with two 6-atom fused rings on each side of V_O^0 , the lengthening of the Si–Si bond following hole trapping is accompanied by a shortening of the Si–second NN oxygen (2nd NN–O) bond lengths by about 0.4–0.5 Å. However, in the case of $V_O(C)$ with two 12-atom fused rings on each side of V_O , there is only a marginal change of the Si–2nd NN–O bond distance for the undistorted side of the cluster around V_O after hole trapping: the other side of the cluster, where a Si atom spontaneously moves away from its position and forms a weak bond with a 3-fold coordinated O center. After hole trapping, the Si (moved)–O (2nd NN–O) bond length increases to a value of about 1.76 Å. One of the 2nd NN–O–Si (moved)–O angles decreases from about 110° to about 99°, while the other two angles deform only slightly. The reason for this change in behavior may be easily understood

by analogy with ring formation in basic carbon chemistry, where it is well-known that 6-atom rings are the most stable, i.e., minimally strained, configuration. In the case of the positively charged vacancies we have studied, the medium vacancy, V_O(B), is already in a 6-atom ring configuration and can only distort by forming a 4-atom ring structure. On the other hand, the large positively charged vacancy, V_O(C), forms a 6-atom ring structure when it deforms.

Interestingly, the ΔE_f (V_O⁺¹) with respect to V_O⁰ (Table 3) is calculated to be about 1.1 eV higher in the case of model V_O(B) than that in V_O(A). However, the value of ΔE_f (V_O⁺¹) in both V_O(A) and V_O(B) is substantially larger, by a factor of 2.5–3 than that in the case of model cluster V_O(C). In fact, the ΔE_f (V_O⁺¹) at the V_O⁰ optimized geometry is calculated to be only 2.83 eV (Table 4). Such a low value of ΔE_f (V_O⁺¹) in the case of model cluster V_O(C) indicates the ease with which an asymmetrically relaxed deep hole trap (E_v') is formed in an oxide network with highly flexible structures.

One also notes that the electron affinity (vertical attachment) of the V_O⁺¹ (asymmetric) at its optimized geometry is about 0.7 eV higher than the vertical ionization potential of the V_O⁰, suggesting the former to be a deep trap center.

Summary

Charge trapping by oxygen vacancy defects in *a*-SiO₂ plays a critical role in determining the electrical properties of thin film semiconductor devices. A microscopic understanding of the structure of these vacancies and the structural changes that accompany charge trapping are essential for improving our fundamental understanding of metal oxide semiconductor (MOS) device physics. To develop such an understanding, we have performed ab initio Hartree–Fock (HF) calculations of the structure and energy of oxygen vacancy sites (V_O) in both neutral (V_O⁰) and positive (V_O⁺¹) charge states using SiO₂ clusters.

Three different precursor clusters were employed in these calculations: (A) a 15-atom cluster without rings; (B) a 39-atom cluster containing four 6-atom (3-membered) rings; and (C) an 87-atom cluster with four 12-atom (6-membered) rings. For precursor clusters A and B, a double- ζ plus polarization (DZP) basis set was used. For cluster C, a minimal (STO-3G) basis set was employed. Our results suggest that the energy of formation, ΔE_f of V_O⁰ and V_O⁺¹ depends on the starting size and geometry of the precursor. Similarly, microscopic structural changes, primarily network relaxation, due to hole trapping by V_O⁰ strongly depend on the initial local structure around the vacancy.

A neutral vacancy, V_O⁰, tends to form a Si–Si dimer bond regardless of the network structure. Similarly, hole trapping at V_O in a relatively rigid network containing 6-atom (3-membered) fused rings results in a small, but symmetric relaxation (i.e., elongation) of the Si–Si bond at the vacancy site. When the

network contains more flexible structures, such as 12-atom (6-membered) rings adjacent to V_O and sufficient asymmetry, trapping of a hole causes an asymmetric relaxation of the two adjacent Si atoms. The asymmetric relaxation in our calculation proceeds without a barrier.

The value of ΔE_f for V_O⁰ and V_O⁺¹ decreases with the flexibility and asymmetry in the oxide network. Results of further studies including 4- and 8-membered rings will be communicated in our forthcoming paper. However, we do not expect the qualitative results of the present study to change significantly.

Acknowledgment. We would like to thank Dr. Rod Devine, Prof. Henry Kurtz, and Prof. Gianfranco Pacchioni for helpful discussions. We would also like to thank the University of New Mexico (UNM) for access to the resources of their Albuquerque High Performance Computing Center (AHPCC) and Maui High Performance Computing Center (MHPCC). The calculations on the small and medium clusters were performed using IBM SP2 and SGI Origin 2000 at AHPCC, MHPCC, and the Aeronautical Systems Center/Major Shared Resource Center (ASC/MSRC). The calculations on the large clusters were performed utilizing the UNM-Alliance Roadrunner Supercluster located at AHPCC under Grant 1999022.

References and Notes

- (1) Fleetwood, D. M.; Riewe, L. C.; Schwank, J. R.; Witzak, S. C.; Schrimpf, R. D. *IEEE Trans. Nucl. Sci.* **1996**, *43*, 2537.
- (2) Fleetwood, D. M.; Winokur, P. S.; Riewe, L. C.; Reber, R. A., Jr. *J. Appl. Phys.* **1998**, *84*, 6141.
- (3) Feigl, F. J.; Fowler, W. B.; Yip, K. L. *Solid State Commun.* **1974**, *14*, 225.
- (4) Rudra, J. K.; Fowler, W. B. *Phys. Rev. B* **1987**, *35*, 8223.
- (5) Boero, M.; Pasquarello, A.; Sarnthein, J.; Car, R. *Phys. Rev. Lett.* **1997**, *78*, 887.
- (6) Griscom, D. L.; Frieble, E. J. *Phys. Rev. B* **1986**, *34*, 7524.
- (7) Tohmon, R.; Shimogaichi, Y.; Tsuta, Y.; Munekuni, S.; Ohki, Y.; Hama, Y.; Nagasawa, K. *Phys. Rev. B* **1990**, *41*, 7258.
- (8) Vanheusden, K.; Stesmans, A. *J. Appl. Phys.* **1993**, *74*, 275.
- (9) Zhang, L.; Leisure, R. G. *J. Appl. Phys.* **1996**, *80*, 3744.
- (10) Conoley, J. F. Jr.; Lenahan, P. M. *IEEE Trans. Nucl. Sci.* **1995**, *42*, 1740.
- (11) Chavez, J. R.; Karna, S. P.; Vanheusden, K.; Brothers, C. P.; Pugh, R. D.; Singaraju, B. K.; Devine, R. A. B. *IEEE Trans. Nucl. Sci.* **1997**, *44*, 1799.
- (12) Karna, S. P.; Pineda, A. C.; Shedd, W. M.; Singaraju, B. K. In *Silicon-on-Insulator Technology and Devices IX (Proceedings Volume 99-3)*; Hemment, P. L. F., Ed.; The Electrochemical Society: Pennington, NJ, 1999; p 161.
- (13) Warren, W. L.; Lenahan, P. M.; Robinson, B.; Stathis, J. H. *Appl. Phys. Lett.* **1988**, *53*, 482.
- (14) Zvanut, M. E.; Feigl, F. J.; Fowler, W. B.; Rudra, J. K.; Caplan, P. J.; Poindexter, E. H.; Zook, J. D. *Appl. Phys. Lett.* **1989**, *54*, 2118.
- (15) Warren, W. L.; Lenahan, P. M. *J. Appl. Phys.* **1989**, *66*, 5488.
- (16) Schmidt, M. W.; Baldrige, K. K.; Boatz, J. A.; Elbert, S. T.; Gordon, M. S.; Jensen, J. H.; Koseki, S.; Matsunaga, N.; Nguyen, K. A.; Su, S. J.; Windus, T. L.; Dupuis, M.; Montgomery, J. A. *J. Comput. Chem.* **1993**, *14*, 1347.
- (17) Snyder, K. C.; Fowler, W. B. *Phys. Rev. B* **1993**, *48*, 13238.